Acta Neuropathol (1996) 92 : 331–340

REGULAR PAPER

John W. Haycock · Peter Jones · John B. Harris
David Mantle

Differential susceptibility of human skeletal muscle proteins to free radical induced oxidative damage: a histochemical, immunocytochemical and electron microscopical study in vitro

Received:31 October 1995 / Revised, accepted: 19 February 1996

Abstract In this study we describe a novel experimental approach to quantify the relative susceptibility of (membrane-associated, contractile and mitochondrial) proteins in normal human muscle tissue sections to oxidative damage by the reactive oxygen species (ROS), hydroxyl (OH·) or superoxide ($O_2.^-$) radicals. The latter species were generated under controlled experimental conditions in vitro using a ^{60}Co gamma radiation source, with subsequent analysis of damage to target proteins (dystrophin, β-dystroglycan, β-spectrin, fast and slow myosin heavy chain, NADH tetrazolium reductase, succinate dehydrogenase and cytochrome oxidase) via standard histochemistry, immunocytochemistry and electron microscopy of muscle tissue sections. In general terms, each of the proteins listed above was more susceptible to oxidative damage by OH·, compared to $O_2\cdot^-$. Different proteins (differing in structure, function or intracellular localisation) showed different susceptibility to oxidative damage, with certain mitochondrial proteins (succinate dehydrogenase, cytochrome oxidase) showing particular susceptibility. In addition, the use of monoclonal antibodies to four different regions of dystrophin showed the latter to contain both resistant and susceptible regions to ROS induced oxidative damage. At the ultrastructural level of subcellular organelle damage, mitochondria were identified as being particularly susceptible to ROS induced oxidative damage. We therefore speculate that oxidative damage to mitochondria and/or mitochondrial proteins may represent the principal initial route of free radical-induced damage within skeletal muscle tissue.

Key words Oxygen free radicals · Proteins · Skeletal muscle · Mitochondria

J. W. Haycock · J. B. Harris · D. Mantle
Muscular Dystrophy Group Research Laboratories,
Regional Neurosciences Centre, Newcastle General Hospital,
Newcastle upon Tyne NE4 6BE, UK

P. Jones
School of Chemistry,
University of Newcastle upon Tyne NE1 7RU, UK

D. Mantle (✉)
Department of Neurochemistry, Regional Neurosciences Centre,
Newcastle General Hospital, Newcastle upon Tyne NE4 6BE, UK
Tel. +0191-273 8811, ext. 22 167; Fax: +0191 226 0775

Introduction

Oxygen free radicals (reactive oxygen species; ROS) are highly reactive transient chemical species (characterised by the presence of unpaired electrons) formed during normal aerobic cellular metabolism (e.g. during electron flux through the mitochondrial electron transport chain). ROS have the potential to initiate damage to the various intracellular components, including nucleic acids, lipids and proteins, on which normal cell functioning depends [9]. The principal ROS of physiological relevance are the hydroxyl (OH·) and superoxide ($O_2\cdot^-$) radicals, respectively. These are ubiquitous in aerobic cell metabolism [9, 18] and cellular damage resulting from the action of these species has been implicated in the pathology of a diverse range of disorders [22, 23], including muscular dystrophy [16]. Muscle tissue is unique in its requirement and ability to undertake very rapid and coordinated changes in energy supply and oxygen flux during contraction, and it has been suggested [28] that this renders the tissue particularly prone to ROS-mediated damage as a result of increased electron flux and corresponding leakage from the mitochondrial respiratory chain. A potential role for ROS in the pathogenesis of human muscular dystrophy was first suggested following the recognition of a form of muscular dystrophy in animals induced by nutritional deficiency of vitamin E and/or selenium [6]. Because of their high reactivity and short half-life, direct analysis of ROS in tissue samples has proved extremely difficult, particularly for in vivo investigations with human subjects [21, 27]. Most of the research into the potential role of ROS in the pathogenesis of muscle disease has therefore been based on indirect analytical methods to quantify ROS-induced damage in experimentally induced or inher-

ited muscle degeneration in animal models. However, a number of problems have become apparent in the interpretation of such data, on which the hypothesis of ROS involvement in muscular dystrophy pathology has been based. These include (1) the choice of unsuitable animal models of relevance to human muscular dystrophy, e.g. the dystrophic chicken [38], which is now known to result from a different genetic defect to that responsible for muscular dystrophy in man [5]; (2) the indirect quantification of ROS-induced damage by estimation of lipid peroxidation products via the thiobarbituric acid-coupled reaction [36], the methodology of which is now known to be subject to artefact [34]. Such difficulties in data interpretation are further compounded by the fact that relatively little is known about the basic mechanisms by which cells are damaged by ROS, particularly their action on key structural and enzymic proteins on which the function of the cell depends.

In view of the above problems, we have adopted an alternative experimental approach to investigation of the role of ROS in muscle cellular damage, based on ROS generation under controlled experimental conditions in vitro using a ^{60}Co γ-radiolysis source, with subsequent analysis of target protein damage in muscle tissue sections via histochemical, immunocytochemical and electron microscopical techniques. A similar experimental approach has been successfully applied to the investigation of ROS-induced oxidative damage in vitro to model proteins (in purified form) such as albumin [11–14, 35] and lysozyme [17]; however, little is known about ROS-induced oxidative damage of muscle proteins, particularly in tissue sections where the cellular architecture has been maintained. The objectives of the work described in this paper were therefore: (1) to determine whether muscle proteins which differ in structure, function or intracellular localisation (membrane-associated, contractile, mitochondrial) may have different relative susceptibilities to ROS-induced oxidative damage; (2) to determine the relative capacity of $OH\cdot$ and $O_2\cdot^-$ radicals to cause oxidative damage to proteins in (1) above. In the longer term, such information identifying the most susceptible targets to ROS-induced oxidative modification and most damaging ROS species within the muscle cell may prove of value in devising novel therapeutic strategies (e.g. based on ROS-scavenging compounds) with potential for the treatment of human patients with muscle-wasting disorders [20, 43].

Materials and methods

Unless otherwise specified, chemicals and reagents were obtained from Sigma (Poole, UK) and were of analytical grade where available.

Preparation of sections

Human quadriceps femoris muscle, obtained (with ethical approval) at open biopsy from three patients with no history of muscle disease, undergoing routine surgery, was correctly orientated for histochemical cryosectioning and flash frozen in thawing isopentane (–150° C) within 10 min of removal, taking care to avoid freezing artefact. Samples were subsequently transferred into a liquid nitrogen storage facility at -196° C for long-term storage. Muscle samples were analysed using standard histochemical screening procedures [30] to confirm the absence of neuropathy or myopathy. For histochemistry, 10-μm-thick frozen transverse muscle sections were made using a cryostat (Leitz Wetzlar, model 1720) at –20° C. Sections were mounted on chromic acid-cleaned slides. For immunocytochemistry, 6-μm-thick frozen transverse muscle sections were made as above, and mounted on gelatinised slides (0.5% w/v gelatin, 0.05% w/v chrome alum) and allowed to air-dry at room temperature for 1 h. For electron microscopy, muscle samples were orientated and cut under tension as described previously [10]. For each biopsy sample, experimental procedures described to quantitate levels of various proteins in irradiated tissue sections were carried out in triplicate.

ROS generation via Co^{60} γ-radiolysis

The protocol outlined below for the generation of $OH\cdot$ or $O_2\cdot^-$ in vitro via ^{60}Co γ-radiolysis of aqueous solutions is based on that of Davies [11], in which both theoretical and methodological aspects of the procedure are described.

For protein solutions in the μM-mM concentration range, damage induced by γ irradiation results primarily from the action of free radical species (not via direct radiative damage). Whilst it is possible to accurately control the concentration of individual (purified) proteins (on which the majority of γ-radiolytic studies have been carried out), it is clearly more difficult to define effective protein target levels (and hence direct radiative damage) during γ-irradiation of whole tissue sections. However, in the present study since irradiation experiments are carried out under identical conditions, the potential contribution of direct radiative damage would be similar for each protein type. In addition, the contribution of direct radiative damage to the overall protein damage process must be relatively small, since (1) tissue sections exposed to different gassing (N_2O/O_2) regimes (which would not affect direct radiative damage) show markedly different levels of damage to target proteins after irradiation; (2) preliminary studies showed incorporation of free radical scavengers (e.g. 1 mM glutathione) in the irradiation medium reduces the extent of subsequent protein damage. It follows that protein damage in tissue sections under the experimental conditions described results primarily from the action of free radical species, and not via direct radiative damage. Quantification of ROS dosage (equivalent to 99 krad·h^{-1}) was via standard dosimetric techniques [19].

Experiments were carried out in which tissue sections were exposed to high (2371 krad), intermediate (1778 krad) and low (1186 krad) ROS dosages, respectively. For generation of $OH\cdot$ radicals, slide-mounted tissue sections were placed into plastic slide containers (Cellpath, Hemel Hempstead, UK) and completely immersed in 100 mM KH_2PO_4/K_2HPO_4 buffer pH 7.5 at 25° C, previously gassed to saturation with N_2O and irradiated as above. For generation of $O_2\cdot^-$ radicals the procedure was as described above, except that the slide immersion buffer contained 20 mM sodium formate (as an $OH\cdot$ scavenger) and was gassed to saturation with O_2. Samples for electron microscopy were placed in 20 ml buffer in Universal containers and gassed and irradiated as above. Additional samples processed as above but not irradiated served as appropriate controls for light or electron microscopy, respectively.

Histology/histochemistry

Tissue sections exposed to $OH\cdot$ or $O_2\cdot^-$ radicals, and respective non-irradiated controls, for haematoxylin and eosin staining were fixed in formol-calcium solution for 15 min at room temperature, thoroughly washed in water, incubated in Lillie Meyers haematoxylin for 1 min and washed in water until blue. They were then immersed in eosin for 1 min, washed in water, and serially dehydrated in ethanol (70%, 95% and 100%). Dehydrated sections were

cleared (Histo-Clear, National Diagnostics, Atlanta, Ga.) and mounted on to coverslips using an organic mounting medium (DPX, BDH, UK).

For histochemical analysis of tissue sections (irradiated/control), cytochrome oxidase activity was determined by the method of Seligman et al. [45] using diaminobenzidine as electron donor and cytochrome *c* as substrate, NADH tetrazolium reductase activity was determined by the method of Pearse [42] using MTT as electron acceptor, and succinate dehydrogenase activity determined by the method of Johnson [1, 30].

Immunocytochemistry

The following monoclonal antibodies (mAbs) were provided by Dr. L. Anderson, MDGB Laboratories, Newcastle upon Tyne, UK and were used to label the proteins dystrophin, 43kDa dystrophin-associated glycoprotein (β-dystroglycan, 43 DAG) and β-spectrin, respectively: DY10/12B2 (dystrophin amino terminus residues 308-351 [41], DY4/6D3 (dystrophin central rod domain residues 1181–1388 [39]), CDYS3/21C1 (dystrophin central rod domain residues 2592–3026 [33], DY8/6C5 (dystrophin carboxyl terminus residues [32, 40]), 43 DAG/8D5 (β-dystroglycan, carboxy terminus residues 880–894 [26]) and RBC2/3D5 (β-spectrin from red cell membranes [4]). mAbs used to label myosin fast and slow heavy chains were provided by Dr. Wendy Brown, Jefferson Medical College, Pennsylvania [available commercially (NCL-MHCF, NCL-MHCS) from Novocastra Laboratories, Newcastle upon Tyne, UK]. Tissue sections were examined by indirect immunofluorescence, following exposure to ROS; sections were incubated with undiluted mAbs for 1 h at 25° C. mAbs were removed by washing with TBST (0.122% w/v TRIS, 0.876% w/v NaCl, 0.05% v/v Tween, corrected to pH 8.1 with concentrated HCl) for 3 × 15 min, and the sections incubated with a secondary immunolabel, rhodamine-conjugated rabbit anti-mouse antibody (R270, Dakopatts, Denmark) for 1 h (diluted 1 : 100 with TBST). Non-specific binding was suppressed by including 3% bovine serum albumin (BSA; BDH, UK) and 0.1M lysine in the antibody diluent. Sections were again washed for 3 × 15 min with TBST, before being mounted on to glass coverslips using an aqueous mounting media (Uvinert, BDH, UK).

Fluorescent photomicrographs were obtained using a photomicroscope equipped with epifluorescence illumination filter for rhodamine (Nikon HFX-II), using a × 40 oil immersion objective lens. Rhodamine is excited by light at 555 nm and emits light at 580 nm, permitting the visualisation of each protein of interest. Ilford 35 mm HP5 Monochrome film was exposed to each of the control samples (400 ASA), using an automatically timed exposure for each control sample (Nikon FX-35DX camera). Corresponding irradiated samples were photographed under the same conditions as their corresponding controls. Photomicrographs of NADH tetrazolium reductase and cytochrome oxidase were obtained using a × 20 objective lens. Monochrome film (Ilford 35 mm PanF 50 ASA) was exposed as above.

Electron microscopy

After irradiation, muscle (held under tension) was cut into 2 mm × 1 mm blocks using a stereo microscope, with the 2-mm axis parallel to the longitudinal orientation of the muscle fibres, and the blocks fixed in 5% glutaraldehyde in 0.1 M phosphate buffer pH 7.4 for 1 h. After rinsing in buffer for 15 min, the muscle was processed for secondary fixation in 1% osmium tetroxide in 0.1 M phosphate buffer for 2 h, with further rinsing in buffer (10 min) and distilled water (10 min), then stained with 4% aqueous uranyl acetate for 20 min. Following serial dehydration in aqueous ethanol (50%, 70%, 90%) muscle blocks were embedded in araldite resin and allowed to set for 24 h. Sections for viewing under the electron microscope were cut at approximately 70 nm using a microtome (Reichert).

Results

Experiments to investigate the relative susceptibility of muscle proteins to ROS-induced oxidative degradation in tissue sections were carried out using irradiation dosages of 1100, 1800 and 2400 krad respectively. Comparison of haematoxylin and eosin stained control and irradiated tissue sections showed no evidence of gross changes in muscle morphology following exposure to OH· or $O_2\cdot^-$ radicals over the above irradiation dose range (data not shown). It was, however, possible to demonstrate ROS-induced damage to specific muscle proteins using appropriate immunocytochemical or histochemical tissue section visualization procedures. The results of a typical experiment (at 2400 krad) to investigate ROS-induced oxidative damage to the sarcolemmal-associated protein dystrophin [24], with immunocytochemical visualisation of the target protein using monoclonal antibodies recognising different protein domains, is shown in Fig. 1. Clear differences in fluorescent staining intensity were evident between skeletal muscle sections exposed to OH· radicals, compared to corresponding non-irradiated controls; this was particularly evident for dystrophin visualisation using monoclonal antibody DY10/12B2 specifically recognising the N-terminal region of the protein (Fig. 1 a, e), and to a somewhat lesser extent using monoclonal antibodies CDYS3/21C1 (recognising part of the central rod region, Fig. 1 c, g) and DY8/6C5 (recognising the carboxy-terminal region of the protein, Fig. 1 d, h), respectively. There was little difference in fluorescent staining intensity between irradiated and non-irradiated tissue sections when dystrophin was visualised using monoclonal antibody DY4/6D3 to the central rod domain of the protein (Fig. 1 b, f). Following exposure to an equivalent dosage (2400 krad) of $O_2\cdot^-$ radicals, differences in fluorescent staining intensity between irradiated (Fig. 1 m–p) and non-irradiated (Fig. 1 i–l) tissue sections were reduced compared to those noted above following exposure to OH· radicals, for corresponding monoclonal antibodies used to label dystrophin protein. Following exposure of tissue sections to $O_2\cdot^-$ radicals, it was of note that the greatest change in immunolabelling staining intensity (compared to non-irradiated controls) was evident when dystrophin was labelled with monoclonal antibody DY8/6C5 (carboxy terminal region, Fig. 1 l, 1 p), compared to that observed following dystrophin visualisation following immunolabelling with monoclonal antibodies DY10/12B2 (Fig. 1 i, m), DY4/6D3 (Fig. 1 j, n) and CDYS3/21Cl (Fig. 1 k, o).

Of the other membrane-associated proteins investigated, a similar pattern of relative susceptibility to oxidative damage by OH· and $O_2\cdot^-$ radicals to that described above for dystrophin was noted for β-spectrin; thus substantial oxidative modification of the protein following exposure to OH· radicals (2400 krad) was evident following visualisation with mAb RBC2/3D5 (Fig. 2 b, f), whereas exposure of tissue sections to an equivalent dose of $O_2\cdot^-$ radicals showed little change in fluorescent immunolabelling intensity compared to non-irradiated con-

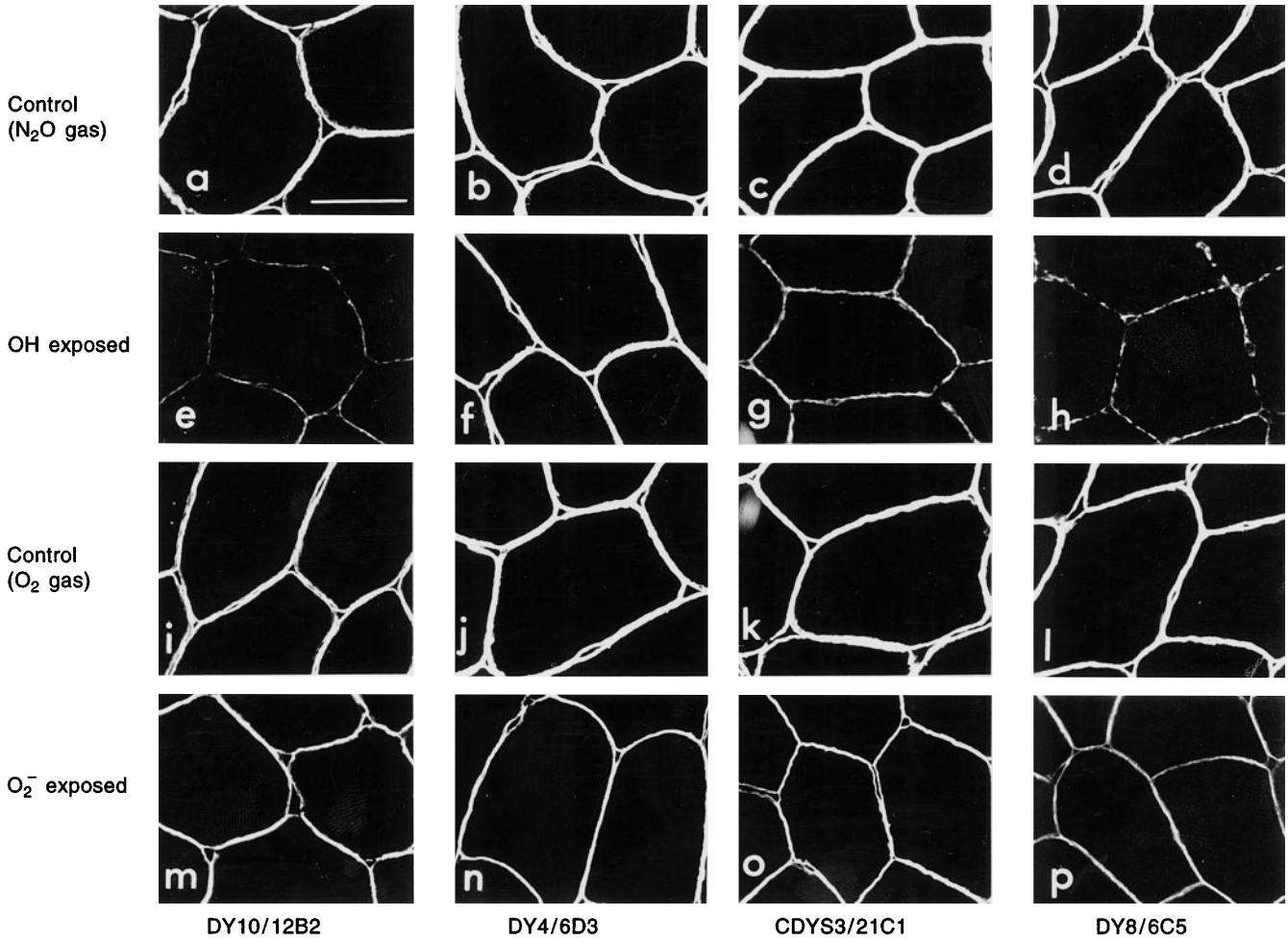

Fig. 1 a–p Changes in immunocytochemical labelling of dystrophin protein following exposure of muscle tissue sections to OH· or O_2·⁻ radicals. **e–h** Tissue sections exposed to OH· radicals, **a–d** corresponding non-irradiated control sections, **m–p** tissue sections exposed to O_2·⁻ radicals, **i–l** corresponding non-irradiated control sections. **a, e, i, m** Monoclonal antibody (mAb) DY10/12B2 recognising NH_2-terminal protein sequence, **b, f, j, n** mAb DY4/6D3 recognising central rod domain protein sequence, **c, g, k, o** mAb CDYS3/21Cl to rod domain sequence, **d, h, l, p** mAb DY8/6C5 to carboxy-terminal protein sequence. The illustrations shown (and in subsequent figures) are randomly selected areas taken from larger photographs of tissue serial sections

trols (Fig. 2 j, n). For the membrane-associated β-dystroglycan, there was little change in staining intensity (with protein visualisation using mAb 43 DAG/8D5) between irradiated and non-irradiated tissue sections following exposure to OH· (Fig. 2 a, e) or O_2·⁻ (Fig. 2 i, m) radicals, respectively.

Similarly, visualisation of the contractile protein myosin (using mAbs to heavy chains from fast and slow isoforms) showed a substantial reduction in immunolabelling following exposure of tissue sections (2400 krads) to OH· radicals (Fig. 2 c, g, d, h), with the degree of protein oxidative damage being reduced following exposure of tissue sections to an equivalent dose of O_2· radicals (Fig. 2 k, o, l, p).

Of those proteins visualised histochemically, the mitochondrial associated enzymes succinate dehydrogenase, cytochrome oxidase and NADH tetrazolium reductase showed differing susceptibility to oxidative damage induced by OH· or O_2·⁻ radicals. Thus the activity of succinate dehydrogenase was completely destroyed in tissue sections exposed to equivalent dosage (2400 krad) of either OH· (Fig. 3 c, f) or O_2·⁻ (Fig. 3 i, j); the activity of cytochrome oxidase was completely destroyed following exposure to OH· (Fig. 3 b, e) and unaltered following exposure to O_2·⁻ (Fig. 3 h, k), whilst the activity of NADH tetrazolium reductase was relatively resistant to damage by both OH· (Fig. 3 a, d) or O_2·⁻ (Fig. 3 g, j).

For tissue sections exposed to OH· or O_2·⁻ at a lower dose of 1800 krad, changes in immunocytochemical or histochemical staining intensities for corresponding proteins were qualitatively similar, but quantitatively of reduced extent, to those described above. Following exposure of tissue sections to OH· or O_2·⁻ at a dose of 1100 krad, no differences in immunocytochemical or histochemical staining intensities were noted for any of the individual protein types investigated. Data detailing the dose dependency of protein damage by OH· and O_2·⁻ for the individual proteins investigated are summarised in Table 1.

The ultrastructural organization of non-irradiated control muscle in oxygen-saturated buffer is shown via elec-

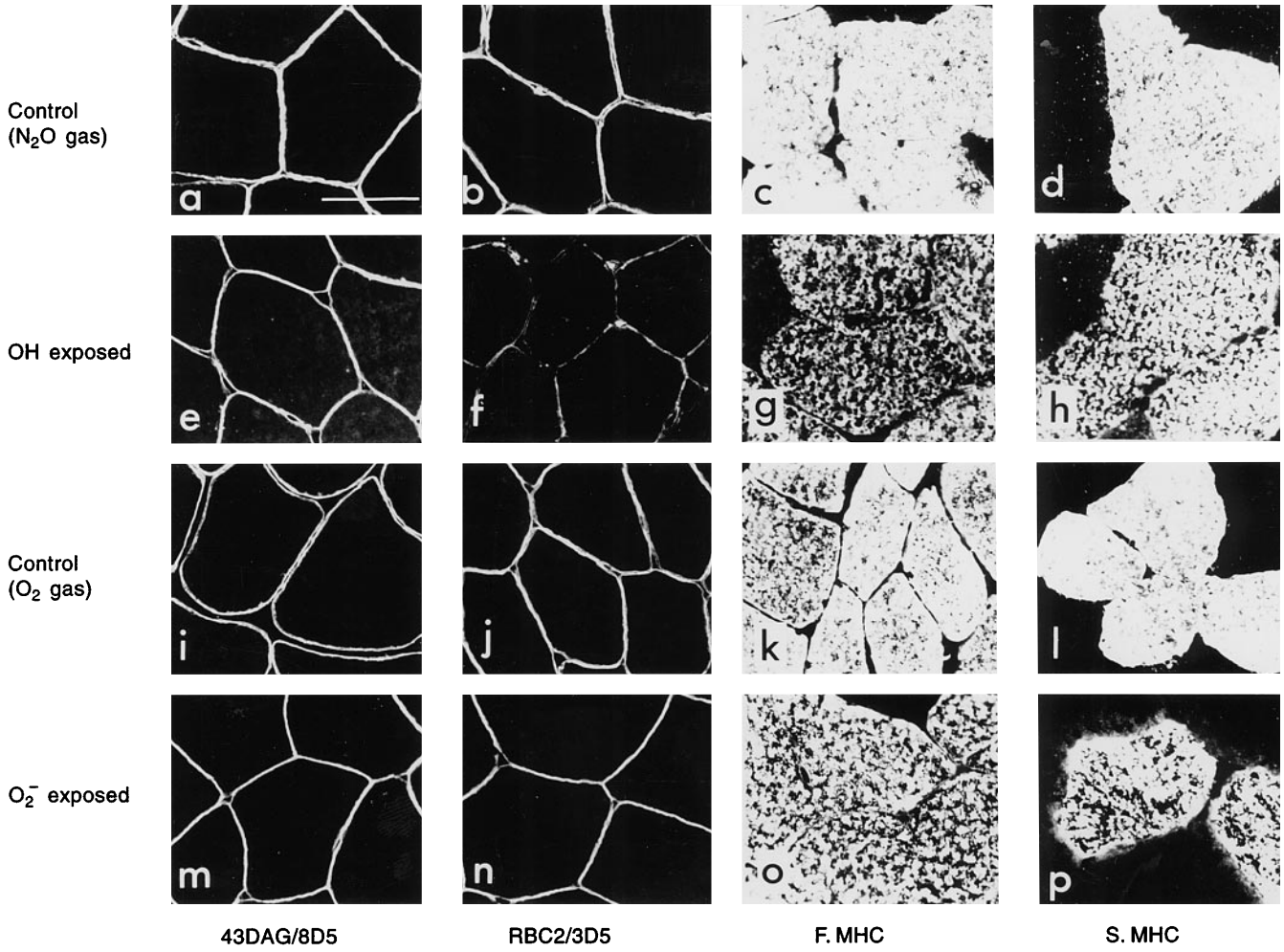

Fig. 2 a–p Changes in immunocytochemical labelling of β-dystroglycan, β-spectrin and myosin following exposure of muscle sections to OH· or O_2·⁻ radicals. **e–h** Tissue sections exposed to OH·, **a–d** corresponding non-irradiated control sections, **m–p** tissue sections exposed to O_2·⁻, **i–l** corresponding non-irradiated controls sections. **a, e, i, m** Monoclonal antibody (mAb) 43 DAG/8D5 recognising carboxyterminal region of β-dystroglycan, **b, f, j, n** mAb recognising β-spectrin, **c, g, k, o** mAb to myosin heavy chain (fast isoform), **d, h, l, p** mAb to myosin heavy chain (slow isoform)

tron microscopy in Fig. 4 a, which shows the distinct muscle tissue banding pattern corresponding to normal morphological criteria i.e. with Z-lines, A-bands and I-bands in register and running at right angles to the myofibrillar long axis, with the myofibrils aligned in a regular manner and sarcomeres present in well defined units; mitochondria with intact inner and outer membranes lie between the myofibrils located either side of the Z-bands. The sarcoplasmic reticulum (SR) and T-system ensheathe the myofibrils and form characteristic triads at the junction of the A- and I-bands. The plasma membrane is located on the outside of the muscle fibres, immediately beneath the external basement lamina which is associated with the endomysial connective tissue. Following exposure to O_2·⁻ radicals (300 krad), the most striking changes in ultrastructure were those relating to the mitochondria. At relatively low magnification (7500 ×), an apparent random distribution of alterations which indicate swelling of this organelle is evident (Fig. 4 b). Considerable variations in mitochondrial size are present, ranging from those with the same cross-sectional area as those in control non-irradiated muscle samples, to those with a size approximately 25 times (i.e. profile area) compared to those found in control samples. Closer examination at higher magnification reveals early disappearance of the characteristic shape of the cristae, with general disorganisation of the inner membrane being evident in the slightly swollen mitochondria. The outer membrane at this stage appears to be intact. More severe damage is represented by a greater swelling of the mitochondria (Fig. 4 c) and myofibrillar distortion is evident. These larger, randomly isolated organelles still contain an outer membrane, but the inner membrane is completely disrupted, resulting in the formation of intramitochondrial vacuoles. Other subcellular regions appear to have empty spaces in the place of once present mitochondria. It is possible that a critical maximum volume is tolerated by mitochondria; once this is exceeded, rupturing of the outer membrane might be expected, resulting in "bursting" and formation of small vacuolar spaces. The action of O_2·⁻ radicals on the muscle ultrastructure ap-

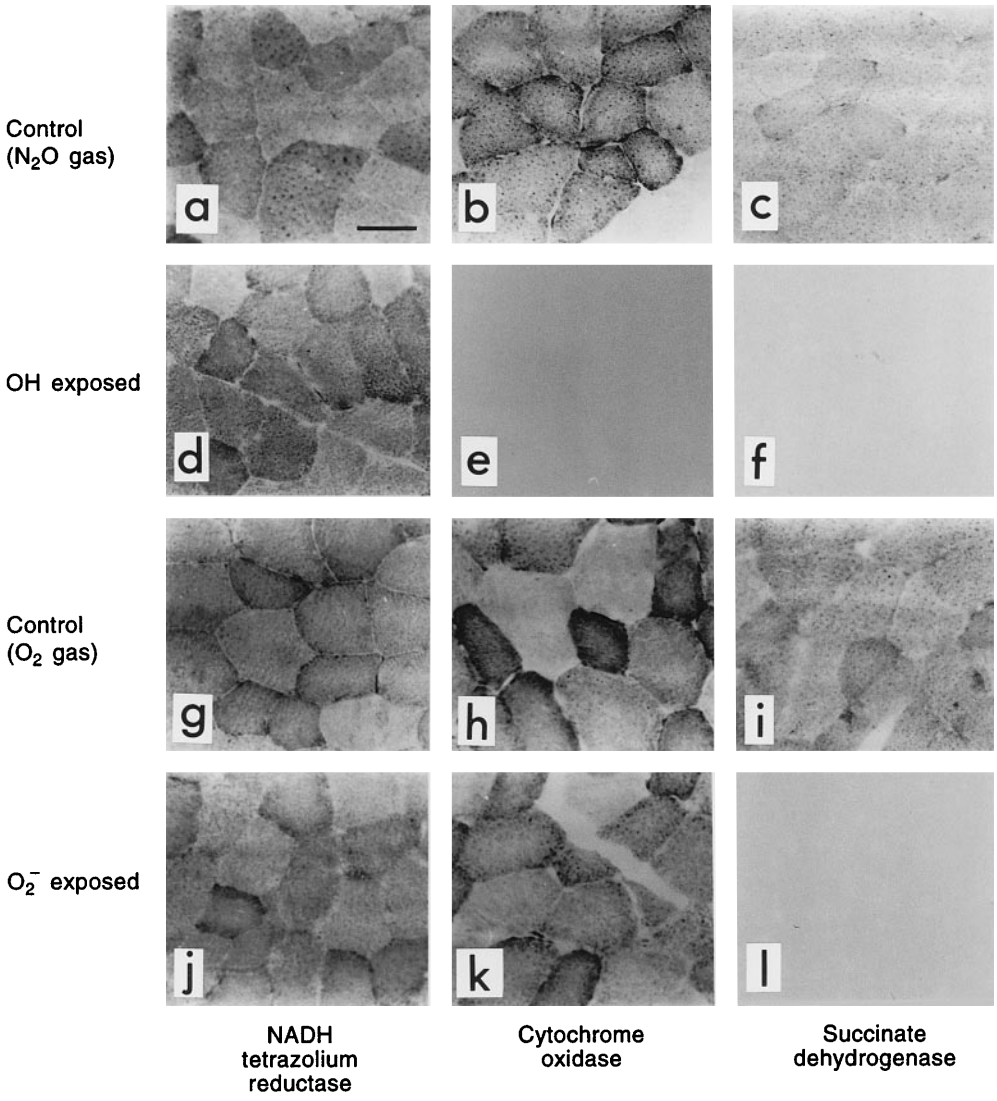

Fig. 3 a–l Changes in histochemical staining of mitochondrial associated enzymes following exposure of tissue sections to OH· or O_2·$^-$. **d–f** Tissue sections exposed to OH·, **a–c** corresponding non-irradiated control sections, **j–l** tissue sections exposed to O_2·$^-$, **g–i** corresponding non-irradiated controls. **a, d, g, j** Histochemical staining for NADH tetrazolium reductase, **b, e, h, k** staining for cytochrome oxidase, **c, f, i, l** staining for succinate dehydrogenase

pears to be selective for mitochondria, and alterations to other subcellular components of the muscle are not evident. The position and size of the T-tubules and SR are not altered, although swollen mitochondria are noted to physically displace the whole triadic structure. Minor alterations in the regular banding pattern of Z-lines, M-band and A-band were noted, but the regular sarcomeric repeats and definition were essentially maintained, and no alteration in the structurre of the plasma membrane was evident.

Investigation of ultrastructural modifications to muscle tissue by O_2·$^-$ radicals were restricted to a maximum dosage of 300 krad, since incubation of muscle samples in oxygen-saturated buffer for longer than 4 h induced alterations to mitochondria (slight swelling, occasional vacuolar spaces) without irradiation. Similarly, investigation of ROS-induced damage at the ultrastructural level was restricted to O_2·$^-$, since incubation of muscle tissue samples in N_2O-gassed buffer (necessary for generation of OH·) for more than 30 min induced widespread and extensive damage to mitochondria without irradiation.

In the various experiments described above, similar data were obtained, using biopsy samples from different patients, in the determination of relative susceptibility of corresponding protein types to oxidative damage by OH· or O_2·$^-$ radicals.

Discussion

During normal aerobic metabolism, the principal source of ROS within the cell results from the leakage of electrons from the mitochondrial respiratory chain – it has been estimated that 3–5% of total electron flux results in the formation of ROS [8]. In addition, ROS are generated by the catalytic action of other membrane associated and cytoplasmic enzymes, e.g. the action of xanthine oxidase in oxidising xanthine to uric acid during purine metabolism, and the inactivation of catecholamines via monoamine oxidase; ROS are also generated during the oxidation of arachidonic acid by lipoxygenases and phagocyte activation during inflammation/infection, and in the de-

Table 1 Changes in immunocytochemical and histochemical labelling of proteins in muscle tissue sections following exposure to OH· or O_2·- radicals. Changes in protein labelling intensity (compared to non-irradiated control section) were assessed semi-quantitatively following visual inspection — no change in labelling intensity, + small change, ++ moderate change, +++ large change or complete loss of labelling intensity

Protein	Relative change in protein labelling					
	2500 kRad		1800 kRad		1100 kRad	
	OH·	$O_2^{\cdot-}$	OH·	$O_2^{\cdot-}$	OH·	$O_2^{\cdot-}$
Dystrophin						
DY10/12B2	+++	–	+	–	–	–
DY4/6D3	–	+	–	–	–	–
CDYS3/21c1	+++	+	+	–	–	–
DY8/6C5	+++	++	++	+	–	–
β-Dystroglycan						
43DAG/8D5	+	–	+	–	–	–
β-Spectrin						
RBC2/3D5	+++	–	++	–	–	–
Myosin						
heavy chain, fast	+++	++	++	+	–	–
heavy chain, slow	++	+	+	–	–	–
Cytochrome oxidase	+++	–	++	–	–	–
NADH tetrazolium reductase	–	–	–	–	–	–
Succinate dehydrogenase	+++	+++	++	++	–	–

toxification of xenobiotics by cytochrome P_{450} related enzymes [15, 18]. Cells are protected from ROS-induced damage by a variety of endogenous ROS-scavenging proteins (e.g. metallothionines [44], ROS-scavenging enzymes (e.g. catalase, superoxide dismutase, peroxidase) and ROS-scavenging compounds (glutathione, α-tocopherol and ascorbate [7, 15, 18]. Cellular damage arising from an imbalance between ROS-generating and ROS-scavenging systems has been implicated in a diverse range of human diseases, including inflammatory immune disorders, emphysema, cardiac and vascular disease, malignancy and arthritis [22], as well as in the inherited disorders of muscle known collectively as muscular dystrophy [16]. Duchenne muscular dystrophy (DMD) results from an Xp-21 linked genetic defect, manifest by the aberrant production of the sarcolemmal associated protein dystrophin [5, 25]. The mechanism by which absence of this protein results in the degeneration of muscle characteristic of DMD is unknown. It has been suggested that absence of dystrophin results in altered homeostasis of intracellular calcium resulting in excessive generation of ROS via activation of the xanthine dehydrogenase/xanthine oxidase system, and subsequent intracellular oxidative damage [2, 3]. Direct experimental confirmation of such hypotheses is difficult; because of their high reactivity (second-order rate constant 10^6–$10^9 \cdot M^{-1} \cdot s^{-1}$) ROS have very short half-lives (10^{-9}–10^{-4} s), making direct analysis (particularly in man) extremely difficult. The only tech-

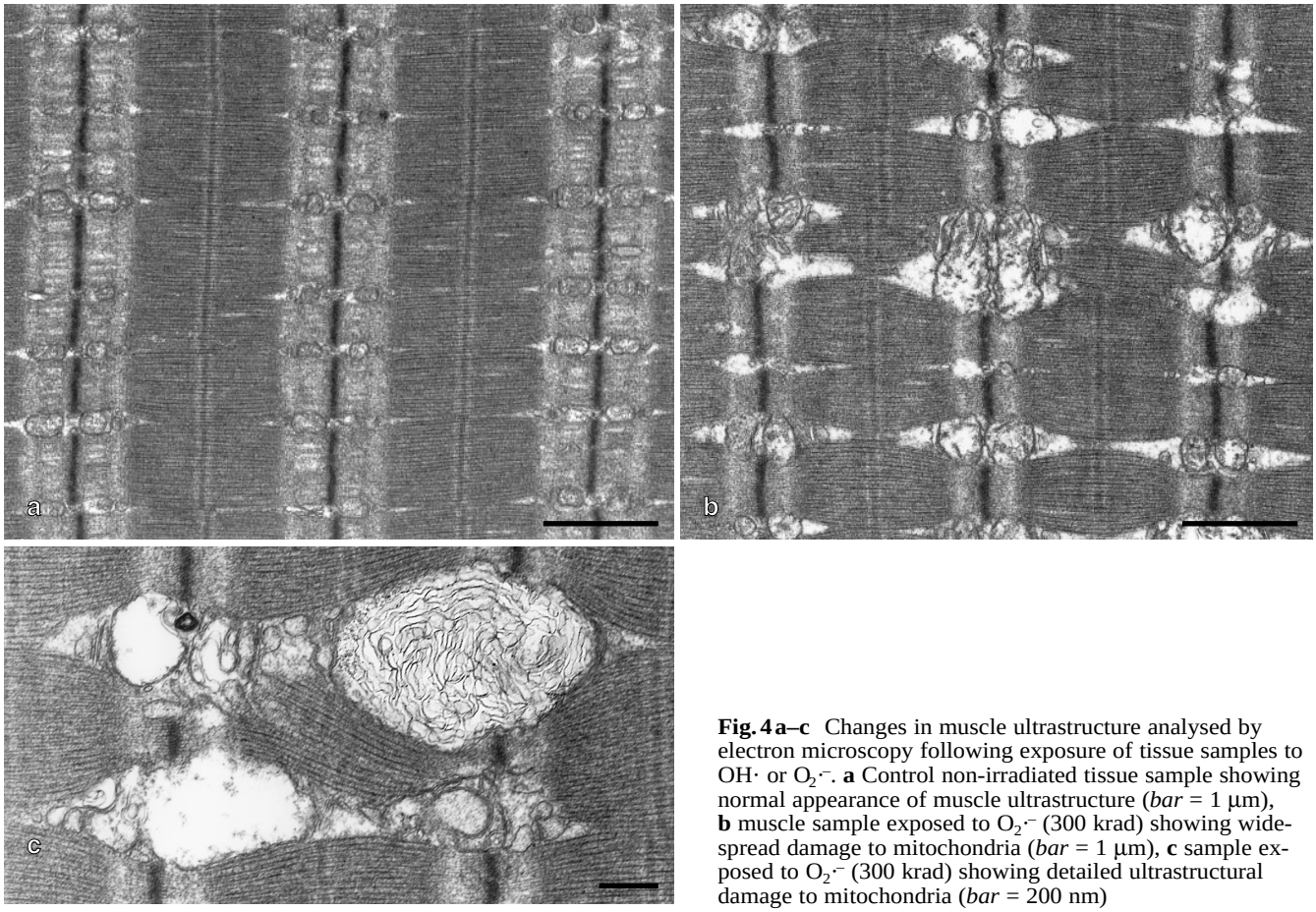

Fig. 4 a–c Changes in muscle ultrastructure analysed by electron microscopy following exposure of tissue samples to OH· or $O_2^{\cdot-}$. **a** Control non-irradiated tissue sample showing normal appearance of muscle ultrastructure (*bar* = 1 μm), **b** muscle sample exposed to $O_2^{\cdot-}$ (300 krad) showing widespread damage to mitochondria (*bar* = 1 μm), **c** sample exposed to $O_2^{\cdot-}$ (300 krad) showing detailed ultrastructural damage to mitochondria (*bar* = 200 nm)

nique capable of direct ROS analysis is that of electron spin resonance (ESR) spectroscopy. This technique is not suitable under all experimental conditions, e.g. it is not possible to measure OH· in aqueous solution at ambient temperature, because of excessive line broadening in the ESR spectrum. Much of the previous research to investigate the potential role of ROS in oxidative damage to muscle tissue has therefore been based on indirect analytical methods to quantify ROS-induced muscle damage (now known to be subject to problems of interpretation and/or inappropriate tissue sampling and use of animal models of human disease, as described in the Introduction).

In view of these problems, we have therefore adopted an alternative experimental approach to investigate the mechanism of ROS-induced oxidative protein damage in human skeletal muscle, based on the generation of ROS in vitro via ^{60}Co γ-radiolysis of muscle tissue sections. There are a number of potential methods for generating ROS in vitro, and the relative advantages and disadvantages of these are reviewed by Stadtman [46]; for the work described in this investigation, generation of ROS via γ-radiolysis was chosen because of the degree of radical specificity and quantification of dosage possible. A similar experimental approach has been successfully applied to the investigation of ROS-induced oxidative damage in vitro of purified model proteins such as albumin and lysozyme [11–14, 17] but has not been applied to the investigation of ROS-induced oxidative damage of muscle proteins, particularly cytoskeletal/contractile proteins [46]. In this study, target proteins were selected to represent different functional or locational categories i.e. plasma membrane-associated (dystrophin, β-dystroglycan, β-spectrin), the contractile protein myosin, the mitochondrial-enzymes cytochrome oxidase, and succinate dehydrogenase, and the mitochondrial/sarcoplasmic-enzyme NADH tetrazolium reductase. A particularly novel aspect of this work is the assessment of ROS-induced oxidative damage to proteins in tissue sections, in which the three-dimensional architecture of the muscle cell has been retained, in contrast to investigations using tissue homogenates or single proteins outlined above; to our knowledge, no comparable studies have been reported previously describing the analysis of ROS-induced oxidative protein damage in tissue sections. The levels of free radicals generated in vitro in the present study are likely to be substantially higher than those generated in vivo (intracellular free radical levels in normal or pathological human tissues are presently unknown); however, under such conditions of substantially reduced overall free radical levels, there is no reason why the principle of differential susceptibility of proteins to oxidative damage established in vitro should not equally apply to proteins in vivo.

From the data described in the Results section we would conclude:

1. All muscle proteins investigated were subject to oxidative damage by ROS in a dose-dependent manner; in general terms, ROS-induced oxidative damage to the various protein types in tissue sections was greater with OH· than $O_2{\cdot}^-$ at a corresponding dosage.

2. Different target proteins showed differing relative susceptibility to oxidative damage, depending on the structure, function or intracellular localisation of the protein.

3. Visualisation of dystrophin using mAbs to different molecular domains has suggested that dystrophin protein comprises different molecular regions which are more or less susceptible to ROS-induced oxidative damage, presumably arising from differences in relative amino acid composition and/or differences in protein folding. Whether this results from subtle alteration or major destruction of these protein regions remains to be determined. The progressive loss of the major (427 kDa) dystrophin bands (corresponding to the intact protein) with increasing dosage of OH· or $O_2{\cdot}^-$ has been confirmed via preliminary Western immunoblotting analysis (using the same antibodies as above); however, since no fragmentation product were identifiable, no additional information could be obtained than that derived from immunocytochemistry. In this regard, it is of note that complete fragmentation of other muscle proteins (myosin, actin) with increasing $OH{\cdot}/O_2{\cdot}^-$ dosage is demonstrable via analytical electrophoresis (J. Haycock, unpublished). The particular susceptibility of the carboxyl region of the dystrophin molecule may result from association of the latter with the lipid environs of the plasma membrane (since proteins associated with a lipid environs may be more susceptible to peroxidative damage [22]).

4. At the ultrastructural level of subcellular organelle damage, mitochondria were identified as being particularly susceptible to ROS-induced oxidative damage. To our knowledge, this is the first report describing ROS-induced muscle tissue damage at the ultrastructural level, identified with electron microscopy. However, alteration of mitochondrial ultrastructure following exposure to $O_2{\cdot}^-$ radicals has been cited in work from other groups, using isolated rat liver mitochondria. Damage to these organelles by $O_2{\cdot}^-$ induces characteristic features which are apparently conserved in all of the studies described; this is of particular interest considering the different methods employed for generating superoxide radicals, and the different techniques used for assessment of damage. For example Janzen et al. [29] reported mitochondrial swelling and vacuolar formation in the cristae following CCl_4 intoxication of rat liver mitochondria, assessed by electron microscopy. Similarly, following exposure of a partially purified rat liver mitochondrial fraction to $O_2{\cdot}^-$ radicals, Kakkar et al. [31] reported mitochondrial swelling identified by changes in optical density. These investigations are in agreement with the present findings that mitochondria are subject to a characteristic form of damage resulting from the action of free radicals.

Considering the high lipid content of mitochondria, it is predictable that the latter are targets for ROS-induced damage. The susceptibility of lipids to free radical-mediated peroxidation has been described previously [22]; initiating ROS induce a cascade of self-propagating reactions resulting in large disruption of the lipid structure.

Evidence for such a reaction in the mitochondrial membrane is substantiated by a study reporting the formation of lipid peroxide products following the exposure of mitochondria to ROS [37]; visual inspection of the electron micrographs reveals large scale disruption of the inner membrane, probably resulting from lipid peroxidative reactions within the membrane.

In the present study, accurate control of $O_2\cdot^-$ dosage and sensitivity of the analysis enabled identification of the most susceptible target organelles, under conditions in which three-dimensional cellular architecture was maintained. Clearly, the inner mitochondrial membrane was the most susceptible region of structural damage. However, the lipid membranes of other organelles appear to be structurally normal following exposure to $O_2\cdot^-$ radicals – the T-tubules, SR and plasma membrane are all unaltered in terms of size and shape. The outer mitochondrial membrane maintains ultrastructural integrity, although it is distorted by the degree of swelling. It is possible that the permeability of the other membranes (mentioned above) are altered by $O_2\cdot^-$, impairing their function while remaining "physically normal" under ultrastructural analysis.

Previous attempts to treat DMD patients with ROS-scavenging enzymes or compounds have proved unsuccessful [47]; this may in part result from a lack of understanding of the mechanisms by which ROS cause damage within cells. Data obtained from the present investigation, to identify those protein targets within the muscle cell which are most susceptible to ROS-induced oxidative damage may, in the longer term, lead to improved strategies for anti-oxidant based treatment of DMD patients.

Acknowledgements We thank the Muscular Dystrophy Group (Great Britain) for financial support (J.W.H., J.B.H.), and Miss Carol Atkinson for preparation of the manuscript.

References

1. Andersen H, Hoyer PE (1974) Simplified control experiments in the histochemical study of coenzyme-linked dehydrogenases. Histochemistry 38:71–83
2. Austin L (1990) How the lack of dystrophin may upset calcium regulation and lead to oxidative damage. In: Kakulas BA, Mastaglia FL (eds) Pathogenesis and therapy of Duchenne and Becker muscular dystrophy. Raven Press, New York, pp 69–82
3. Baker MS, Austin L (1989) The pathological damage in Duchenne muscular dystrophy may be due to increased intracellular oxy-radical generation caused by the absence of dystrophin and subsequent alterations in calcium metabolism. Med Hypoth 29:187–193
4. Bewick GS, Nicholson LVB, Young C, O'Donnell E, Slater CR (1992) Different distributions of dystrophin and related proteins at nerve-muscle junctions. Neuro Report 3:857–860
5. Bonilla E, Samitt CE, Miranda AF, Hays AP, Salviati G, Di Mauro S, Kunkel LM, Hoffmann EP, Rowland LP (1988) Duchenne muscular dystrophy: deficiency of dystrophin at the muscle cell membrane. Cell 54:447–452
6. Bradley R, Fell BF (1980) Myopathies in animals. In: Walton JN (ed) Disorders of voluntary muscle, 3rd edn. Churchill Livingstone, London, pp 824–872
7. Buettner GR (1993) The pecking order of free radicals and antioxidants: lipid peroxidation, α-tocopherol and ascorbate. Arch Biochem Biophys 300:535–543
8. Chance B, Sies H, Boveris A (1979) Hydroperoxide metabolism in mammalian organs. Physiol Rev 59:527–605
9. Cheeseman KH, Slater TF (1993) An introduction to free radical biochemistry. Br Med Bull 49:481–493
10. Cullen MJ, Mastaglia FL (1980) Morphological changes in dystrophic muscle. Br Med Bull 36:145–152
11. Davies KJA (1987) Protein damage and degradation by oxygen radicals. I. General aspects. J Biol Chem 262:9895–9901
12. Davies KJA, Delsignore ME (1987) Protein damage and degradation by oxygen radicals. III. Modification of secondary and tertiary structure. J Biol Chem 260:9908–9907
13. Davies KJA, Delsignore ME, Lin SW (1987) Protein damage and degradation by oxygen radicals. II. Modification of amino acids. J Biol Chem 262:9902–9907
14. Davies KJA, Lin SW, Pacifici RE (1987) Protein damage and degradation by oxygen radicals. IV. Degradation of denatured protein. J Biol Chem 262:9914–9920
15. Del Maestro RL (1980) An approach to free radicals in medicine and biology. Acta Physiol Scand 492:153–168
16. Dunn JF, Frostick S, Brown G, Radda GK (1991) Energy status of cells lacking dystrophin: an in vivo/vitro study of mdx mouse skeletal muscle. Biochim Biophys Acta 1096:115–120
17. Franzini E, Sellak H, Hakim J, Pasquier C (1993) Oxidative damage to lysozyme by the hydroxyl radical: comparative effects of scavengers. Biochim Biophys Acta 1203:11–17
18. Freeman BA, Crapo JD (1982) Biology of disease. Free radicals and tissue injury. Lab Invest 47:412–426
19. Fricke H, Hart EJ (1966) Radiation dosimetry (Attix FH, Roesch WC (eds) Academic Press, New York, pp 167
20. Hall ED, Andrus PK, Yonkers PA (1993) Brain hydroxyl radical generation in acute experimental head injury. J Neurochem 60:588–594
21. Halliwell B, Grootveld M (1987) The measurement of free radical reactions in humans. Some thoughts for future experimentation. FEBS Lett 213:9–14
22. Halliwell B, Gutteridge JMC (1989) Lipid peroxidation: a radical chain reaction. In: Halliwell B, Gutteridge JMC (eds) Free radicals in biology and medicine, 2nd edn. Oxford University Press, New York, pp 1988–276
23. Halliwell B, Gutteridge JMC (1990) Role of free radicals and catalytic metal ions in human disease: an overview. Methods Enzymol 186:1–85
24. Harris JB, Cullen MJ (1992) Ultrastructural localisation and the possible role of dystrophin. In: Kakulas BA, McHowell J, Roses AD (eds) Duchenne muscular dystrophy: animal models and genetic manipulation. Raven Press, New York, pp 19–40
25. Hoffman EP, Brown RH, Kunkel LM (1987) Dystrophin: the protein product of the Duchenne muscular dystrophy locus. Cell 51:919–928
26. Ibraghimov-Beskrovnaya O, Ervasti JM, Leveille CJ, Slaughter CA, Sernett SW, Campbell KP (1992) Primary structure of dystrophin-associated glycoproteins linking dystrophin to the extracellular matrix. Nature 355:696–702
27. Jackson MJ, Jones DA, Edwards RHT (1984) Techniques for studying free radical damage in muscular dystrophy. Med Biol 62:135–138
28. Jackson MJ, O'Farrell S (1993) Free radicals and muscle damage. Brit Med Bull 49:630–641
29. Janzen EG, Towner RA, Yamashiro S (1990) The effect of phenyl tert-butyl nitrone on CCl_4 induced rat liver injury detected by proton magnetic resonance imaging in vivo and electron microscopy. Free Radic Res Commun 9:325–335
30. Johnson MA (1991) Applications of enzyme histochemistry in muscle pathology. In: Stoward PJ, Pearse AEG (eds) Histochemistry (vol 3) 4th edn. Churchill Livingstone, London, pp 489–514
31. Kakkar P, Mehotra S, Viswanathan PN (1992) Interrelation of active oxygen species, membrane damage and altered calcium functions. Mol Cell Biochem 111:11–15
32. Koenig M, Monaco AP, Kunkel LM (1988) The complete sequence of dystrophin predicts a rod-shaped cytoskeletal protein. Cell 53:219–228

33. Lemaire C, Heilig R, Mandel JL (1988) The chicken dystrophin cDNA: striking conservation of the C-terminal coding and 3′ untranslated regions between man and chicken. EMBO J 7:4157–4162
34. Marshall PJ, Warso MA, Lands WE (1985) Selective microdetermination of lipid hydroperoxides. Anal Biochem 145:192–199
35. Marx G, Chevion M (1985) Site-specific modification of albumin by free radicals. Biochem J 236:397–400
36. Mechler F, Imre S, Dioszeghy P (1984) Lipid peroxidation and superoxide dismutase activity in muscle and erythrocytes in Duchenne muscular dystrophy. J Neurol Sci 63:279–283
37. Mehotra S, Kakkar P, Viswanathan PN (1991) Mitochondrial damage by active oxygen species in vitro. Free Radic Biol Med 10:277–285
38. Muzuno KOY (1988) Pathogenesis of progressive muscular dystrophy: studies on free radical metabolism in an animal model. Acta Neurol Scand 77:108–114
39. Nicholson LVB, Davison K, Falkous G, Harwood C, O'Donnell E, Slater CR, Harris JB (1989) Dystrophin in skeletal muscle: I. Western blot analysis using a monoclonal antibody. J Neurol Sci 94:125–136
40. Nicholson LVB, Davison K, Johnson MA, Slater CR, Young C, Bhattacharya S, Gardner-Medwin D, Harris JB (1989) Dystrophin in skeletal muscle: II. Immunoreactivity in patients with Xp21 muscular dystrophy. J Neurol Sci 94:137–146
41. Nicholson LVB, Johnson MA, Bushby KMD, Gardner-Medwin D, Curtis A, Ginjaar IB, Den Dunnen JT, Welch JL, Butler TJ, Bakker E, Van Ommen GB, Harris JB (1993) Investigation of 100 patients with Xp21-linked muscular dystrophy: integrated analysis using clinical, genetic, immunocytochemical and histopathological data. J Med Genet 30:728–736
42. Pearse AGE (1972) Histochemistry, theoretical and applied, 3rd edn. Churchill Livingstone, London
43. Rangan U, Bulkley GB (1993) Prospects for treatment of free radical-mediated tissue injury. Br Med Bull 49:700–718
44. Sato MS, Bremner I (1993) Oxygen free radicals and metallothionen. Free Radic Biol Med 14:325–337
45. Seligman AM, Karnovsky MJ, Wasserkrug HK, Hanker JS (1968) Non-droplet ultrastructural demonstration of cytochrome oxidase activity with a polymerising osmiophillic reagent, diamino benzidine (DAB) J Cell Biol 38:1–14
46. Stadtman ER (1990) Metal ion-catalysed oxidation of proteins: biochemical mechanism and biological consequences. Free Radic Biol Med 9:315–325
47. Stern LZ, Ringel SP, Ziter FA, Menander-Hubek K, Ionasescu V, Pellecirino RJ, Snyder RD (1982) Drug trial of superoxide dismutase in Duchenne muscular dystrophy. Arch Neurol 39:342–346